11th International Conference on Marine Technology
MARTEC 2018

ASSESSMENT OF DRAG PENALTY RESULTING FROM THE ROUGHNESS OF FRESHLY CLEANED AND PAINTED SHIP-HULL USING COMPUTATIONAL FLUID DYNAMICS

Muhammad Luqman Hakim[1], Bagus Nugroho[2], Rey Cheng Chin[3], Teguh Putranto[1], I Ketut Suastika[1] and I Ketut Aria Pria Utama[1*]

[1]Department of Naval Architecture,
Institut Teknologi Sepuluh Nopember,
Surabaya, Indonesia, 60111
[2] Department of Mechanical Engineering,
The University of Melbourne,
3010 Victoria, Australia
[3] School of Mechanical Engineering,
The University of Adelaide,
5005 South Australia, Australia

ABSTRACT

A Study of Computational Fluid Dynamics (CFD) to assess the impact of rough surface from a recently cleaned and painted ship hull will be reported. The rough surface is obtained through surface imprint during its annual dry docking and digitised via laser scanner. Closer inspection reveals that freshly coated ship hull exhibits an "orange peel" surface roughness pattern with physical height ranging from 0.1 mm – 0.5 mm. Such roughness height would influence the turbulent flow dynamics, elevating ship's drag penalty. Our initial CFD results for two ships show that such surface would cause an increase of skin friction coefficient of full scale ship by 33% - 35%, which corresponds to an increase in the ship's total resistance by 7.5% - 28%. The type of ship that is most affected by the roughness is a ship that has higher frictional resistance ratio compared to residual resistances or it has lower Froude number.

Keywords: *Surface roughness; Drag penalty; Computational Fluid Dynamics; Frictional Resistance; freshly cleaned and painted ship hull.*

1.0 INTRODUCTION

In the last decade the rising cost of fuel prices and the issue of global warming have sparked much interest in finding ways to reduce energy consumption, particularly in the marine transportation industry. Recent reports show that around 100,000 ships operating worldwide consume around 200-300 metric tons of fuel, contributing towards 11% of Green House Gases (GHG) emission compared to other mode of transportations [1][2][3]. To minimise this negative effect, the International Maritime Organization (IMO) and International Council on Clean Transportation (ICCT) has issued regulations to reduce emissions in the form of rules and guidelines to promote more environmentally friendly ships [4][5][6]. There have been many efforts by the industry to reduce ship's energy usage and GHG, including a more efficient engine, sulphur fuel abatement technology, etc. (see [7] for recent reviews).

A significant amount of energy consumption on a large bulk carrier is to overcome skin-friction drag to propel the ship forward. It is estimated up to 80%-90% of the total drag experienced by a large bulk carrier is due to turbulent skin-friction drag [8]. This issue

*Corresponding author: kutama@na.its.ac.id

is made worse by the existence of hull surface roughness. Such roughness is generally caused by biofouling or hull imperfection [9-14]. Hull imperfections generally arise from repeated cleaning (scrapping, water blasting, or sand blasting) and painting process (anti corrosion and antifouling paints) during dry docking. Closer examination to this surface reveals a noticeable roughness that is above the ideal smooth condition. Recent reports also show that even a recently cleaned and painted ship hull may still suffer from an elevated drag penalty due to hull imperfections [13] [15].

In this report, a Computational Fluid Dynamic (CFD) study is performed to investigate the effects of a recently cleaned and painted ship hull are made. The hull roughness is obtained via imprint and digitised using a laser surface scanner. From the results, we are able to scale the drag penalty into a full scale ship.

2.0 SKIN FRICTION DRAG DUE TO ROUGHNESS

For practicing naval architects, obtaining an accurate prediction in ship's resistance is critical, as it forms the basis of the engine power for the ship to sail at the desired speed. Ship resistance consists of friction resistance, and residual resistance. This resistance will include the skin frictional resistance and part of the pressure resistance force. While residual resistance is usually dominated by wave resistance in the case of ships in general. The resistance components can be formulated in a non-dimensional form as follows [16]:

$$C_T = C_F + C_R = C_F + C_{VP} + C_W = (1+k)C_F + C_W \quad (1)$$

Where C_T is the total resistance coefficient, C_F is the frictional resistance coefficient, C_R is the residuary resistance coefficient, C_{VP} viscous pressure resistance coefficient, C_W is the wave resistance coefficient and (1+k) is hull shape coefficients.

Skin friction coefficient (C_F) can be predicted by the wind or water tunnel experimental test on flat plate. The numerical CFD simulation can also be chosen to determine the value of C_F. From CFD software, the resistance value of model can be generated and then the C_F value can be obtained using the following:

$$C_F = R/\frac{1}{2}\rho S U_e^2 \quad (2)$$

where R is the value of the resistance obtained from the experiment or CFD, ρ is the density of fluid, S is the plate surface area, U_e is the freestream velocity relative to surface.

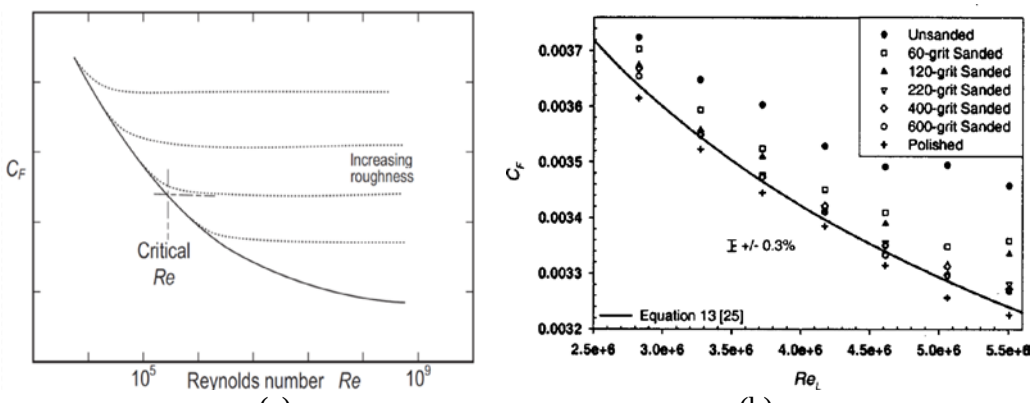

(a) (b)

Figure 1: Relationship between C_F and roughness, a [16], b.[17].

Drag due to rough surface is separation drag behind each individual item of roughness. Turbulent boundary layers have a thin laminar sublayer close to the surface. As Reynolds number increases (for increasing Velocity), the sublayer gets thinner and eventually a point

is reached at which the drag coefficient ceases to follow the smooth turbulent line and becomes approximately constant as in Figure 1, Molland et al [16] and as experimental result by Schultz [17].

3.0 ROUGHNESS GEOMETRY

The surface roughness used in this study is similar with that of Utama et al [13]. Here an imprint made of silicone rubber was taken on the hull of a recently cleaned and painted ship, as in Figure 2a, which looks like an orange peel surface and then it is called the "orange peel" roughness so on. The imprint is later scanned using a laser triangulation sensors Keyence™ LK-031 which is attached to a two-axis computer controlled positioning system. The laser has a vertical (z) and horizontal (x and y) resolution of 1 μm and 60 μm respectively. A geometry of computer-readable roughness was created which will later be used as the CFD numerical model (see Figure 2b). Figure 3 shows the resulting scan which reveal the "orange peel" pattern. Important parameters of the roughness are tabulated in Table 1, where z' is the surface deviation about mean height $z' = z - \bar{z}$.

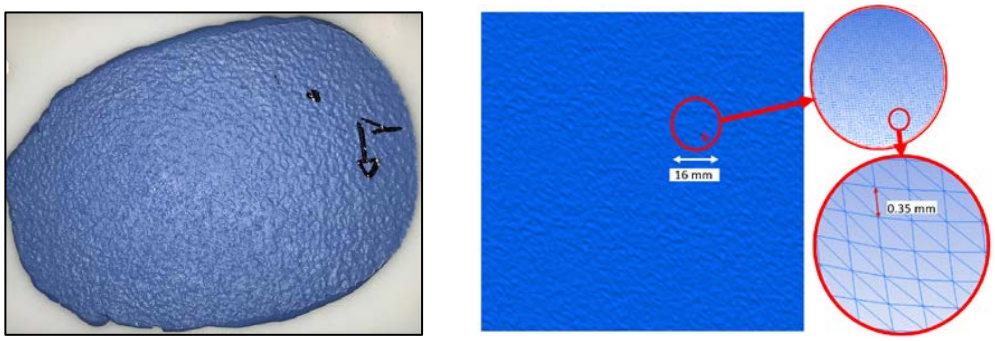

(a) (b)

Figure 2: a. Silicon rubber imprint, b. Roughness geometry in *.stl format.

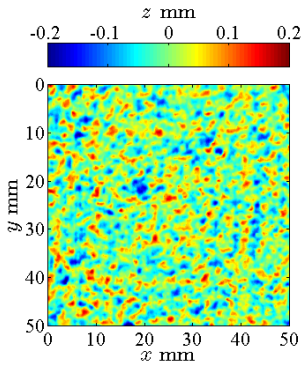

Figure 3: Surface roughness scan.

Table 1: Surface roughness parameters

Parameter	Value	Units	Equation
k_a	0.0413	mm	$\lvert\lvert\bar{z'}\rvert\rvert$
k_{rms}	0.0519	mm	$\sqrt{\overline{z'^2}}$
k_p	0.4791	mm	$\max z' - \min z'$
k_{sk}	0.0868	-	$\overline{z'^3} / k_{rms}^3$
k_{ku}	3.0712	-	$\overline{z'^4} / k_{rms}^4$
ES_x	0.0890	-	$\lvert dz' / dx \rvert$

4.0 NUMERICAL MODELING

4.1 Mathematical formulation

The governing equations that were used in this study is the Unsteady Reynolds-Averaged Navier-Stokes (URANS). The CFD program, FLUENT, is employed to solve of the mass and momentum conservation equations. The turbulent model equation used in the simulations is the SST (Shear Stress Transport) k-ω (see Demirel et al [18] and Menter [19]), where the k-ω model applies in the near wall region and the k-ε for model in the far field for the RANS closure. The SIMPLEC scheme is chosen for pressure-velocity coupling in the solution methods. Spatial discretisation for gradient is least squares cell based and the pressure is second order while the remaining momentum, turbulent kinetic energy and specific dissipation rate are second order upwind.

4.2 Geometry and boundary conditions

There are two computational models, first is the smooth wall, which acts as the reference, and the second is the "orange peel" roughness. The roughness from Figure 2b is applied to a surface plate model (2D like relief) sized B x L = 50 mm x 300 mm. The size is relatively small, but it is chosen with consideration of the computational resources available.

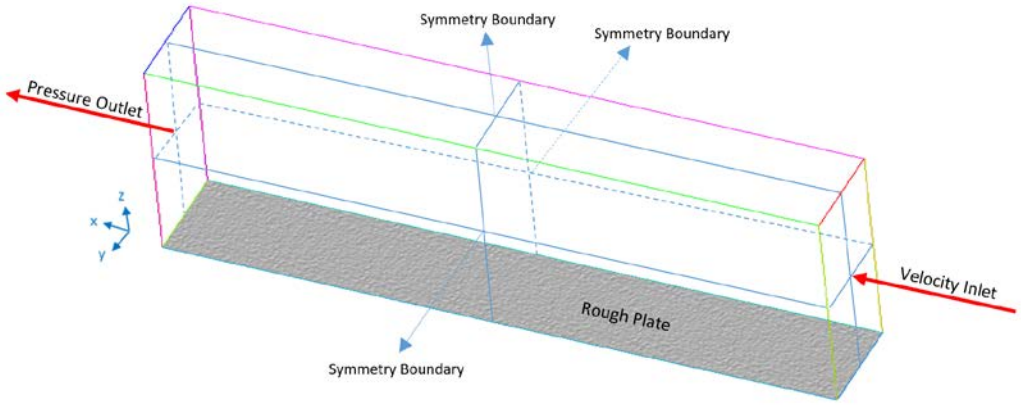

Figure 4: Geometry of computational domain and boundary conditions.

The computational domain is shown in Figure 4. Both the smooth wall and the "orange peel" rough wall has the same grid resolutions. The distance from surface to top boundary is 300 mm. A symmetry boundary condition is imposed on the top and side surfaces. This ensures that the boundary condition has no effect on the calculation (i.e. it can be regarded as free slip wall). The inlet free stream (U_e) is initialised with Reynolds number from 10^5 - 10^{11} using Reynold number formula:

$$U_e = \frac{Re\,\mu}{\rho\,L} = \frac{Re\,\nu}{L} \tag{3}$$

where ρ is the density of the fluid, L is a characteristic linear dimension, μ is the dynamic viscosity of the fluid and ν is the kinematic viscosity of the fluid.

4.3 Mesh generation

Figure 5 shows the appearance of the mesh generation on the plate with the "orange peel" roughness, where it uses structured mesh or also called hexahedral element. It can be seen that the mesh resolution is able to accurately model the "orange peel" roughness. The number of elements made was about 8 million.

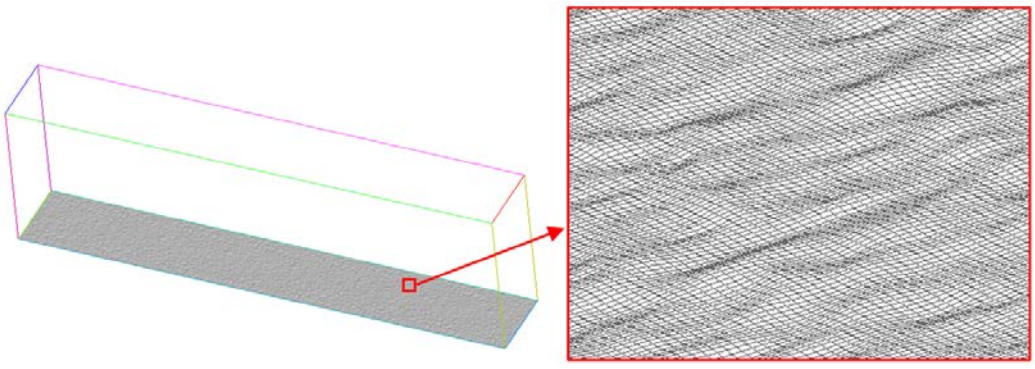

Figure 5: Mesh generation for the "orange peel" roughness model.

Further evidence of the accuracy in modelling the roughness is shown in Figures 6 and 7. In Figure 6, the histogram of the roughness height is shown and the average height

is 0.042mm, which is very close to the 0.0413 mm from the digital scan in Table 1. Figure 7 shows a very similar roughness profile as the digital scan in Figure 3.

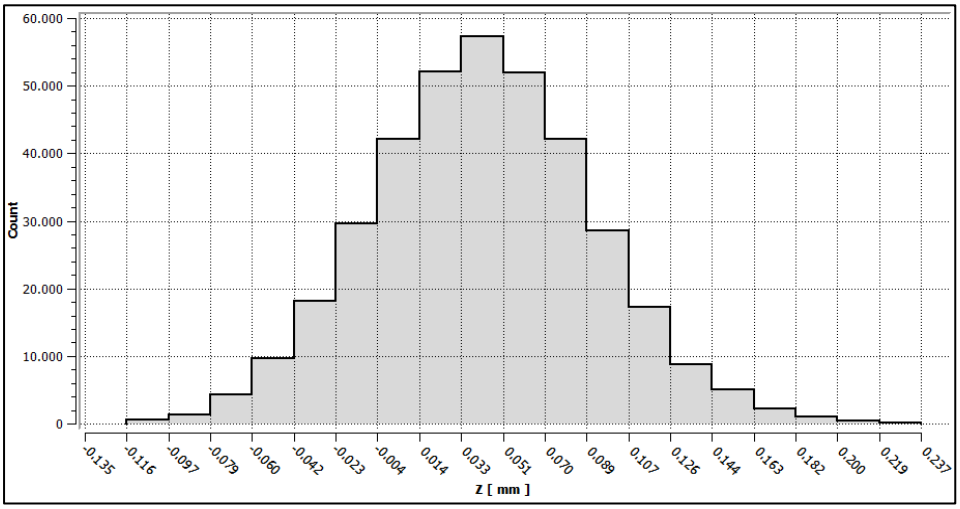

Figure 6: Histogram of mesh height arrangement as roughness.

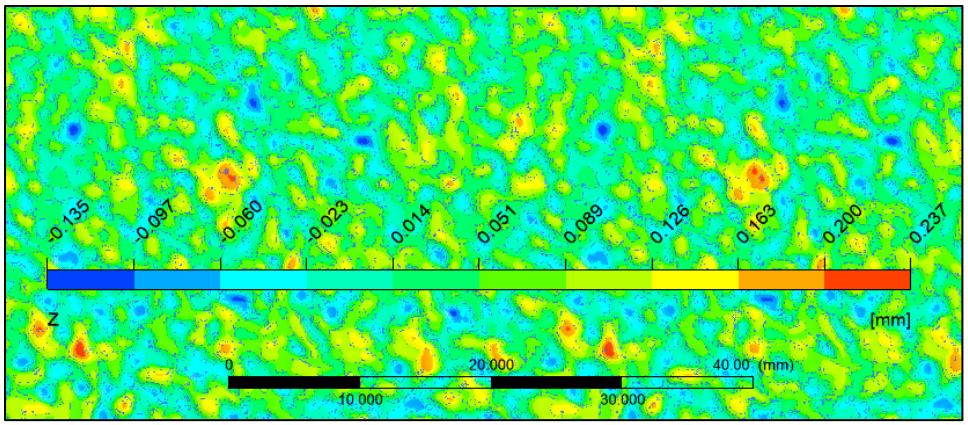

Figure 7: The variation in roughness height in the computational model.

5.0 RESULT

5.1 Increase in C_F value

After performing the numerical simulations of the two models (smooth and rough), the overall friction resistance (R) values are obtained for each free stream variation, and then C_F values for the Reynolds number range of 10^5 - 10^{11} can calculated using Equation 2 and plotted in Figure 8. Both smooth and rough simulation results are also calculated the difference percentage using Equation 4. Where C_{F_S} is for the smooth plate model and $C_{F_{OP}}$ is for the "orange peel" roughness plate model. They are compared with the C_F for smooth wall of Schoenherr [20], shown in Equation 5.

$$\%\Delta C_F = 100x \frac{(C_{F_{OP}} - C_{F_S})}{C_{F_S}}\Big|_{Re} \quad (4)$$

$$\frac{1}{\sqrt{C_F}} = 4.13 \times \mathrm{Log}(Re \times C_F) \quad (5)$$

From Figure 8, it can be seen that C_F of the “orange peel” roughness is higher than C_F of smooth plate and the difference percentage increases with increasing Reynolds number. At Reynolds number about 10^8 there was a drastic increase compared to other Reynolds

number area. According to Molland et al [16] this is an area of critical Reynold number as in Figure 1a.

Here we use the resulting plot to estimate the change in C_F of full scale ships, namely FFG-7 Oliver Perry class frigate and Very Large Crude Carrier (VLCC), with length of 124 m and 320 m, respectively [9][12]. For the FFG-7, the C_F was analysed when the ship is at cruising speed (15 knot) and full speed (30 knot), while the VLCC is at cruise speed only (17 knots). Figure 8 shows that the change in C_F (between smooth wall and rough wall) for FFG-7 at cruise speed is 32.78%, while at full speed is 34.45%. For VLCC, the change in coefficient of friction is 35.52%.

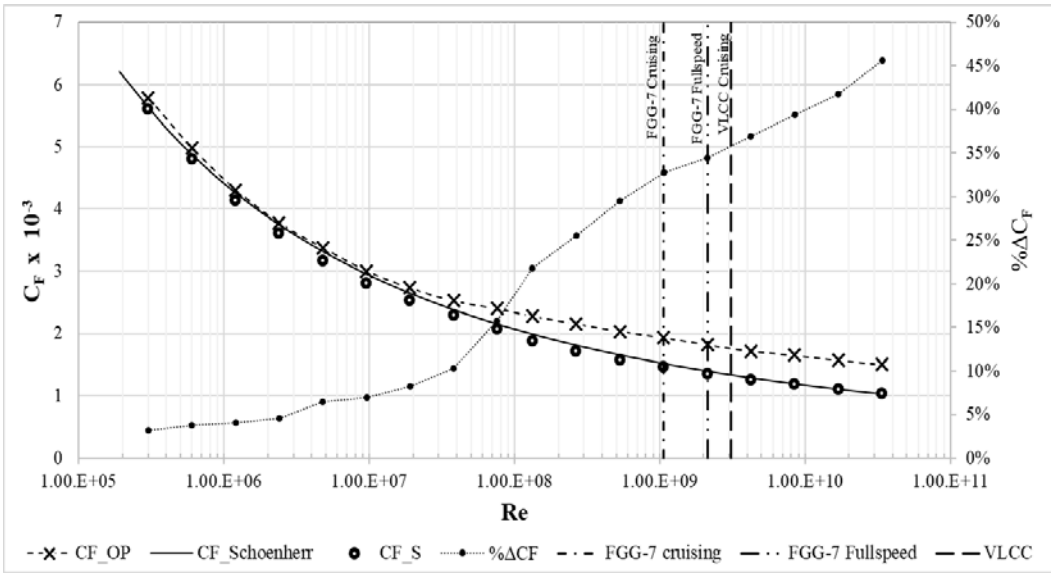

Figure 8: The calculation result of skin friction coefficients C_F against Reynolds number.

5.2 Drag penalty estimation on full scale ships

Following Schultz [9] and Monty et al [12], from Equation 6 we can obtain the ship's total resistance percentage change via:

$$\%\Delta R_T = 100 \times \frac{\Delta C_F}{C_{F_S}\left(1+\frac{C_R}{C_F}\right)+C_A} \tag{6}$$

Where C_R/C_F is the comparison of residual resistance values or wave resistance to the frictional resistance. The purpose of comparing the two vessels in this case is because they have different characteristics of C_R/C_F, where the FGG -7 is designed for high speed vessel and in contrast to VLCC. It can be seen from their Froude number in Table 2. Therefore, it can be concluded that VLCC have more dominant frictional resistance than its wave resistance, and vice versa for FGG-7 vessels. Then C_A is a correction factor released by ITTC [21], where VLCC has a smaller C_A value than that of FGG-7.

Table 2: The estimation the increasing total resistance due to the "orange peel" roughness.

L (m)	C_A	V(knot)		Fr	Re	C_R/C_F	$\%\Delta C_F$	$\%\Delta R_T$
124	0.0004	Cruising	15	0.22	$1.06\text{x}10^9$	~0.7	32.78%	16.6%
		Full-speed	30	0.44	$2.13\text{x}10^9$	~3.3	34.45%	7.5%
320	0.00024	Cruising	17	0.15	$3.10\text{x}10^9$	~0.08	35.52%	28.1%

For the FFG-7, the percentage change in total resistance while it is at cruise and full speed are 16.6% and 7.5% respectively. For the VLCC, its change in total resistance is 28.1%. Detailed information on the calculations and results of the increasing in the total

resistance are tabulated in Table 2. The results demonstrate that even a recently cleaned and painted ship hull, there is still severe drag penalty from hull imperfection.

The type of ship, that is most affected by the roughness to its total resistance, is a ship that has higher frictional resistance ratio compared to its residual resistance. Based on Table 3 [7], it can be seen that tankers, bulk carriers and containers have a higher frictional resistance ratio than catamaran ferry. A ship with the higher C_B, it has the higher wet surface area. Moreover, it can be seen that the lower Froude number also affects the value of C_R/C_F ratio. Therefore, if the ship hull gets roughness, then it will greatly affect the total resistance. The other types of roughness that can also cause the drag penalty, such as: biofouling, anti-fouling coating [22], defect of material or welding, etc.

Table 3: Approximate distribution of resistance components [7].

Type	L (m)	C_B	Dw (tonnes/ TEU)	Serv. speed (Kn.)	*Fr*	Hull resistance component (%)			C_R/C_F
						Frict.	Form	Wave	
Tanker	330	0.84	250000	15	0.136	66	26	8	0.52
Tanker	174	0.80	41000	14.5	0.181	65	25	10	0.54
B. carrier	290	0.83	170000	15	0.145	66	24	10	0.52
B. carrier	180	0.80	45000	14	0.171	65	25	10	0.54
Container	334	0.64	10000	26	0.234	63	12	25	0.59
Container	232	0.65	3500	23.5	0.250	60	10	30	0.67
Cat. ferry	80	0.47	650 pass 150 cars	36	0.700	30	10	60	2.33

6.0 CONCLUSION

CFD simulations have been conducted to determine the increase of C_F values from a recently cleaned and painted hull. Detailed surface scanning shows that the hull surface has "orange-peel" type of roughness ranging from 0.1- 0.5 mm. Initial computational analysis shows that the "cleaned" baseline hull already have a significant drag penalty for large ships, with an estimated increase of 33%-35% in coefficient of friction compared to smooth surface. This in turn results in an increase of 7.5%-28% in total ship resistance. The type of ship that is most affected by the roughness is a ship that has higher frictional resistance ratio compared to other resistance components or it has lower Froude number. Note that the CFD prediction is still preliminary, further studies using a more accurate method such as large eddy simulation (LES) or direct numerical simulation (DNS) are needed to confirm the results.

ACKNOWLEDGEMENTS

The first author wished to thank the Ministry of Research, Technology and Higher Education Republic of Indonesia for funding his study under PMDSU Batch 3 scheme at ITS. Part of the work is funded by ITS through Abdimas 2018 Grants (Contract Number: 1198/PKS/ITS/2018), the Newton Fund Foundation and the British Council and the Australia Research Council.

REFERENCES

1. Corbett, J., Fisbeck, P.S., Pandis, S.N., 1999. Global nitrogen and sulfur inventories for oceangoing ships. *J. Geophys. Res*. 104(D3) 3475 – 3470
2. Erying, V., Isaksen, I., Bemsten, T., Collins, W.J., Corbett, J.J, Endersen, O., Grainger, R.G., Moldavon, J., Schlager, H., Stevenson, D. S., 2010. Transport impacts on atmosphere and climate: Shipping. *Atmos. Environ*., 44(37):4735–4771
3. Wang, H. and Lutsey, N., 2013. *Long-Term PotentiaL for Increased Shipping Efficiency Through the Adoption of Industry-Leading Practices.* Washington: International Council on Clean Transportation (ICCT).

4. IMO., 2005. *The International Convention for the Prevention of Pollution from Ships (MARPOL).*
5. IMO., 2012. *Guidelines on the Method of Calculation of the Attained Energy Efficiency Design Index (EEDI) for new ships.* MEPC.212(63).
6. ICCT., 2011. *The Energy Efficiency Design Index (EEDI) for New Ships*. Washington: International Council on Clean Transportation.
7. Molland, A., Turnock, S., Hudson, D., Utama, I., 2014. Reducing Ship Emissions: A Review of Potential Practical Improvements in The Propulsive Efficiency of Future. *Transactions of the Royal Institution of Naval Architects, Part A2, International Journal of Maritime Engineering (IJME),* Vol. 156, April – June. pp. 175 - 188.
8. Kodama. Y., Kakugawa. A., Takahashi. T., Kawashima., H., 2000. Experimental study on microbubbles and their applicability to ships for skin friction reduction, *Int. J. Heat and Fluid Flow*, Vol.21, pp.582–588.
9. Schultz, M.P., 2007. Efects of coating roughness and biofouling on ship resistance and powering. *Biofouling*, 23:5, 331-341.
10. Schultz, M. P., Bendick, J. A., Holm, E. R., Hertel, W. M., 2011. Economic impact of biofouling on a naval surface ship. *Biofouling*, 27:1, 87-98.
11. Turan, O., Demirel, Y. K., Day, S., & Tezdogan, T. (2016). "Experimental determination of added hydrodynamic resistance caused by marine biofouling on ships". Transportation Research Procedia, Vol. 14(Elsevier), 1649-1658.
12. Monty, JP., Dogan, E., Hanson, R., Scardino, AJ., Ganapathisubramani, B., Hutchins, N. (2016). "An assessment of the ship drag penalty arising from light calcareous tubeworm fouling". *Biofouling*, Vol. 32(4), hal. 451-464.
13. Utama, I., Nugroho, B., Chin, C., Hakim, M. L., Prasetyo, F. A., Yusuf, M., Suastika, I., Monty, J., Hutchins, H., Ganapathisubramani, B., 2017. A Study of Skin Friction-Drag from Realistic Roughness of a Freshly Cleaned and Painted Ship Hull. *Proceed. of International Symposium on Marine Engineering (ISME),* Tokyo, D25-314.
14. Hakim, M., Utama, I., Nugroho, B., Yusim, A., Baithal, M., Suastika, I. (2017). "Review of Correlation between Marine Fouling and Fuel Consumption on A Ship". *Proceeding of SENTA: 17th Conference on Marine Technology.* Surabaya: Institut Teknologi Sepuluh Nopember. pg. II (122-129).
15. Nugroho, B., Baidya, R., Nurrohman, M., Yusim, A., Prasetyo, F., Yusuf, M., Suastika, I., Utama, I., Monty, J., Hutchins, N., Ganapathisubramani, B., 2017. In-situ turbulent boundary layer measurements over freshly cleaned ship-hull under steady cruising. *Proceeding of International Conference on Ship and Offshore Technology (ICSOT), Royal Institution of Naval Architects (RINA) Conference,* Jakarta.
16. Molland, A., Turnock, S., Hudson, D., 2011. *Ship Resistance and Propulsion.* Cambridge: Cambridge university press.
17. Schultz, M. P., 2002. "The Relationship Between Frictional Resistance and Roughness for Surfaces Smoothed by Sanding". *Journal of Fluids Engineering*, Vol. 124 (ASME), 492-499.
18. Demirel, Y. K., Turan, O., Incecik, A., 2017. Predicting the effect of biofouling on ship resistance using CFD. *Applied Ocean Research*, Vol. 62, pp. 100–118.
19. Menter, F.R., 1994. Two-equation eddy-viscosity turbulence models for engineering applications, *AIAA-Journal*, 32(8), pp. 1598 – 1605.
20. Schoenherr, K.E., 1932. Resistance of flat surfaces moving through a fluid. *Transactions of the Society of Naval Architects and Marine Engineers*. Vol. 40.
21. ITTC., 1978. Report of performance committee. *In: Proc. 15th International Towing Tank Conf*, The Hague.
22. Demirel, Y.K., Khorasanchi, M., Turan, o., Incecik, A., Schultz, M.P., 2014. A CFD model for the frictional resistance prediction of antifouling coatings. *Ocean Engineering*, Vol. 89, pp. 21-31.